Aperture Neuro

Maiani M, Hilderley A, Lebel C, Geeraert B, Carlson H, Kirton A. Bilateral differences in structural connectivity of the afferent visual pathways of children with perinatal stroke. *Aperture Neuro*. 2024;4. doi:10.52294/001c.123922

Original Research Articles

Bilateral differences in structural connectivity of the afferent visual pathways of children with perinatal stroke

Meghan Maiani, BScOT[1,2,3], Alicia Hilderley, PhD[1,2,3], Catherine Lebel, PhD[2,3,4], Bryce Geeraert, PhD[2,3], Helen Carlson, PhD[1,2,3], Adam Kirton, MD, MSc, FRCPC[1,2,3,4a]

[1] Department of Pediatrics and Clinical Neurosciences, University of Calgary, [2] Alberta Children's Hospital Research Institute, University of Calgary, [3] Hotchkiss Brain Institute, University of Calgary, [4] Department of Radiology, University of Calgary

Keywords: perinatal stroke, vision, diffusion weighted imaging, tractography, neurodevelopment, stroke, white matter, lesion mapping

https://doi.org/10.52294/001c.123922

Aperture Neuro

Vol. 4, 2024

Objective

Characterize the structural organization of the afferent visual system in children with perinatal stroke (PS).

Background

PS is a leading cause of lifelong disability, including cerebral palsy. Cerebral visual impairment (CVI) is another common outcome, yet mechanisms and developmental plasticity of the visual system after PS are not well understood. CVI can negatively impact how children engage with their environments, consequently affecting development, learning, therapy, play, and future independence.

Methods

Fifty-one children with PS (22 arterial ischemic stroke (AIS), 29 periventricular venous infarction (PVI), mean 10.4 SD 2.5 years) were recruited from a large population-based sample along with 43 typically developing controls (TDC; mean age 11.3, SD 3.5 years). Diffusion weighted images were acquired from all children and the afferent visual tracts (optic chiasm to primary visual cortex) of both hemispheres were isolated using constrained spherical deconvolution (CSD)-based probabilistic tractography. Diffusion metrics of fractional anisotropy (FA) and mean diffusivity (MD) were extracted. Differences in visual pathway microstructure were examined between hemispheres and compared to TDCs.

Results

Both stroke subtypes showed higher MD and lower FA compared to TDC ($p<0.001$) in the lesioned hemisphere and lower FA ($p<0.001$) in the non-lesioned hemisphere. Between-hemisphere differences showed lower FA in the AIS group ($p<0.001$) and higher MD ($p<0.001$) in children with PS.

Conclusion

Visual pathway microstructure is altered in both hemispheres of children with PS, particularly those with AIS. Understanding the structural development of the visual pathways after PS may inform diagnostic, prognostic, and therapeutic strategies.

INTRODUCTION

Perinatal stroke (PS) occurs in 1:1000 births and can result in motor, cognitive, and visual impairments that can affect independence throughout the lifespan.[1,2] PS can be classified as a group of six specific cerebrovascular diseases defined by mechanism and timing of injury.[1] PS occurs between 20 weeks of fetal life and 28 days of postnatal life,

a Corresponding author:
Adam Kirton (adam.kirton@ahs.ca)
Pediatrics and Clinical Neurosciences, University of Calgary

although roughly half of cases are not recognized until they present as motor impairment later in infancy with the remote stroke confirmed by imaging and labelled presumed perinatal stroke. The two most common forms of PS are arterial ischemic stroke (AIS), which occurs most often within the middle cerebral artery and results in large lesions near term, while periventricular venous infarction (PVI) results in smaller lesions and occurs in the midgestational stage.[3] Both stroke types can inflict discrete injuries to posterior visual pathways between the lateral geniculate nucleus (LGN) and visual cortex.

As the leading cause of hemiparetic cerebral palsy (CP), the primary focus of PS research to date has been on motor impairments, where an improved understanding of developmental motor plasticity in both the lesioned and non-lesioned hemisphere has informed new clinical interventions.[4] In contrast, few studies have aimed to explore the mechanisms of visual impairments that complicate PS. Research shows that asymmetry and microstructural differences of the optic radiations may be associated with visual outcomes after AIS when assessed at 3 months of age.[5] Similar microstructural differences in the lesioned hemisphere have been described in children with periventricular and cortico-subcortical lesions with no clear differences between groups.[6] There exists increasingly robust evidence of PS-induced alterations in the development of the non-lesioned hemisphere,[7-10] yet this has not been examined in the visual system.

Cerebral visual impairment (CVI) refers to visual and perceptual deficits resulting from damage to the post-chiasmic pathways of the visual system, including the optic tract and optic radiations. It has been estimated that up to 70% children with cerebral palsy have CVI,[11] and while PS is the leading cause of hemiparetic cerebral palsy, we currently do not know how many children with PS are experiencing CVI. CVI can negatively impact how children interpret visual information and engage with their environment, consequently affecting typical development in activities such as ambulation,[12] social communication,[13,14] and school performance,[15] where even mild visual impairment is associated with decreased socioeconomic status in adulthood.[16] Understanding the structural development of the visual pathways can support the advancement of diagnostic and prognostic tools for visual impairment in children with early brain injury and contribute to development of therapies to reduce functional impairment.

Here, using diffusion weighted imaging and tractography, we aimed to reconstruct the tracts of the afferent visual system in both hemispheres of children with PS and compare them between stroke subgroups and to typically developing controls. We hypothesized that structural development of the afferent visual pathways would be altered bilaterally in children with AIS.

METHODS

PARTICIPANTS

One-hundred and one children aged 6-18 years with PS were recruited from the Alberta Perinatal Stroke Project,[17] a population-based cohort: N=29 AIS (mean age 10.0 [SD 2.9], 12 males), N=29 PVI (mean age 10.2 [SD 3.1], 20 males), N=43 TDC (mean age 11.3 [SD 3.5], 20 males). Stroke group participants (AIS and PVI) were consented as part of a larger study, Stimulation for Perinatal Stroke Optimizing Recovery Trajectory (the SPORT trial)(https://www.clinicaltrials.gov/) and the cross-sectional baseline imaging is used in the current study. Inclusion criteria for the perinatal stroke group were: 1. Age 6–18 years with term birth (>36 weeks), 2. clinical and MRI-confirmed perinatal ischemic stroke (AIS, PVI), 3. symptomatic hemiparetic CP, 4. informed consent/assent. Exclusion criteria included other neurological disorders not related to perinatal stroke, diffuse or multifocal stroke, severe hemiparesis, severe spasticity (Modified Ashworth Scale >3), severe delay or inability to comply with protocol, unstable epilepsy, any MRI contraindication. Similarly aged typically developing controls were recruited via a community healthy controls recruitment database (HICCUP, www.hiccupkids.ca). Inclusion criteria for typically developing children were 1. Term birth, 2. No MRI contraindications, 3. Right-handed. Parental written informed consent and participant assent were acquired. This study was approved by the Conjoint Health Research Ethics Board at the University of Calgary.

NEUROIMAGING ACQUISITION

Images were acquired using a 3T GE MR750w scanner, and a 32-channel head coil, at the Alberta Children's Hospital Diagnostic Imaging Suite in Calgary, Alberta, Canada. Single-shell diffusion images (60 directions, b=2000 s/mm^2, 5 b0 volumes, 2.5mm isotropic voxels, repetition time (TR)/echo time (TE)=15s/87.5ms, duration=16:30 mins) were acquired in the axial plane. T1-weighted anatomical (166 slices, 1mm isotropic voxels, TR/TE=8.5/3.2ms, duration=4:53 minutes) sequences were also obtained in the axial plane.

IMAGE PROCESSING

Diffusion image pre-processing was completed using MRtrix3, SPM, and Synb0.[18-20] Standard diffusion data preprocessing steps were followed including denoising, Gibbs ringing removal, motion and eddy current correction. Synbo-Disco was used to create a synthetic undistorted b=0 image to enable echo planar image distortion correction. Anatomical segmentations were performed using SPM12.[18] Resulting grey matter, white matter, and cerebrospinal fluid masks were combined to create a brain mask. In MRtrix3, fibre orientation distribution (FOD) maps were calculated using the constrained spherical deconvolution model. Subsequently, three-tissue response estimation was completed and used for 3-tissue CSD modelling.[21] Final steps included

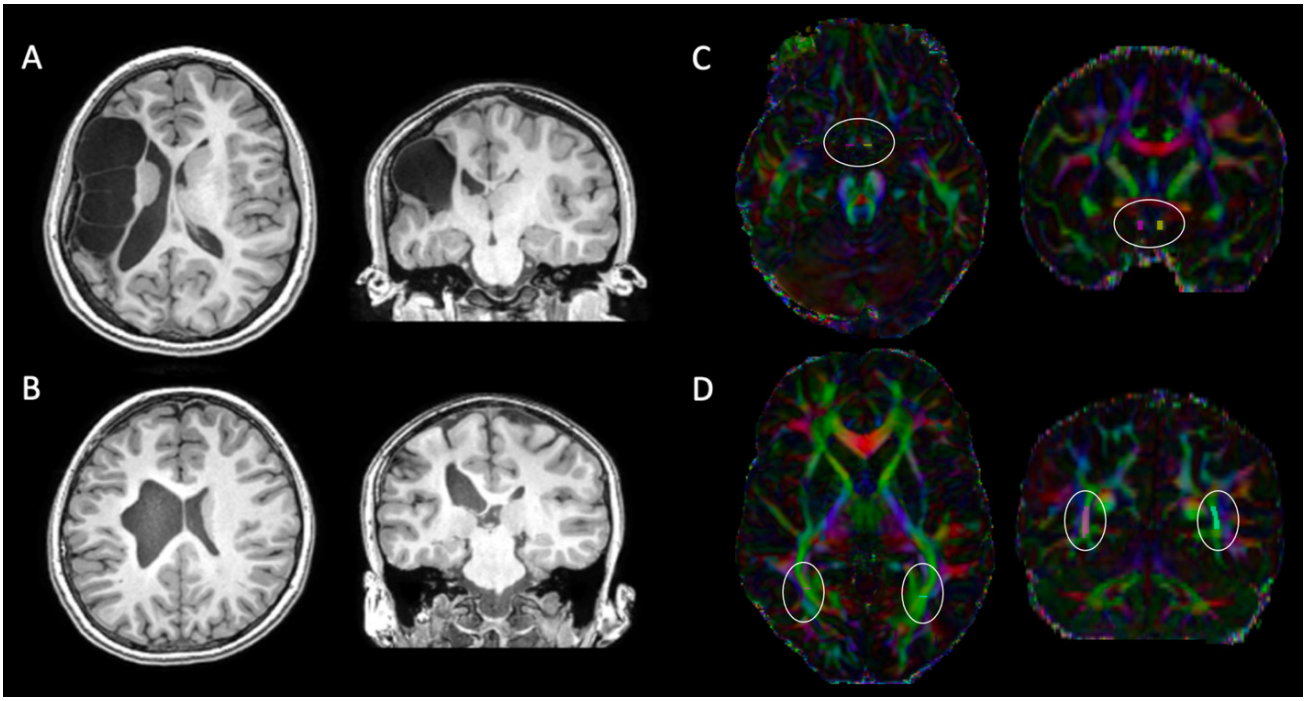

Figure 1. Left: Perinatal stroke subtypes: Arterial Ischemic stroke (A) due to middle cerebral artery occlusion, and periventricular venous infarction (B) in axial (left) and coronal (right) views. Right: An illustration of regions of interest (ROI) locations used to isolate optic radiations. ROI seeds in the anterior optic tract (C) and the optic radiations (D).

bias field correction and multi-tissue informed log-domain intensity normalisation.[22-24]

TRACTOGRAPHY

Probabilistic white matter tractography was completed in MRtrix3[20] to reconstruct the visual pathways in each hemisphere. Two regions of interest (ROI) were defined on coronal slices in each hemisphere [Figure 1, right]. The optic chiasm ROI was drawn on a coronal slice just posterior to the crossing fibres (red on the colour map) of the optic chiasm. The posterior thalamic radiation ROI was drawn on the coronal slice anterior to the splenium of the corpus callosum.[25] Tracts in each hemisphere were reconstructed using the *tckgen* command and the iFOD2 probabilistic algorithm (maximum 5000 streamlines, maximum angle 45^0, stepsize 1.25mm). Participants whose tracts could not be reconstructed within these parameters were excluded. After reconstruction, spurious streamlines and those that were not anatomically plausible as visual tracts were removed using exclude ROIs. Spurious fibres removed included those belonging to the fornix, uncinate fasciculus, and splenium of the corpus callosum. Binary masks were generated from the final tracts and whole-tract mean fractional anisotropy (FA) and mean (MD) diffusivity were extracted in each hemisphere separately.

ALONG THE TRACT METRICS

To more precisely localise regions where white matter microstructure might be affected by lesion damage compared to TDCs, along-tract data extraction was performed. The *tckresample* function of MRtrix3 was used to identify and sample 11 different locations along the optic tract, LGN, and optic radiations (Figure 5A). First, the reconstructed visual tracts and the ROIs from the tractography procedure were overlaid on the colourmap, and a third ROI was added at the LGN. Coordinates were then extracted corresponding to the ROI placements in each hemisphere of each participant to define an arc projecting between the ROIs. For each of the equidistant 11 subsegments of the tract, FA and MD were extracted.

ASSESSING LESION LOCATION AND SIZE

Using T1-weighted anatomical images, lesions were classified by a pediatric neurologist (AK) into PVI and AIS subtypes. AIS lesions were further classified into proximal M1 (n=19), distal M1 (n=9) and lenticulostriate (n=1) vascular territories. To quantify lesion size, lesion masks were created in MRIcron using the 3D paint tool[26] based on T1-weighted image intensity (difference at edge - 8) and consensus was achieved for accuracy of lesion demarcation by a secondary reviewer (HC). As PVI lesions often appear as enlarged ventricles, ventricular volume was calculated for both right and left hemispheres using the same procedure as above, and the ventricle volume of the non-lesioned hemisphere was subtracted from the lesioned hemisphere. Lesion volume was calculated from the binary lesion masks using FSL via *fslmaths*.[27] To identify which along-tract segments were in close proximity to stroke lesions for the AIS group, tracts were overlaid on the coregistered image for

Table 1. Demographic and anatomical characteristics of participant groups

Characteristics by participant group	AIS (N=22)	PVI (N=29)	TDC (N=43)	P-values
Age - mean (SD) years [min-max]	10.0 (2.9) [6.6-19.5]	10.2 (3.1) [7.4-13.9]	11.3 (3.5) [7.3-18.8]	0.09
Sex - N [%]				
Male	N=12 [54.5%]	N=20 [69.0%]	N= 25 [58.1%]	0.67
Female	N=10 [45.4%]	N=9 [31.0%]	N= 18 [39.5%]	
Stroke hemisphere - N [%]				
Left	N=15 [68.1%]	N=15 [51.7%]	-	
Right	N=7 [31.8%]	N=14 [48.2%]	-	

Table note: SD – Standard deviation, AIS – Arterial ischemic stroke, PVI – Periventricular venous infarction, TDC – Typically developing controls

each participant and each tract subsegment was coded as to whether it was colocalized with the lesion (1) or not (0).

STATISTICAL ANALYSIS

Statistical analyses were completed using Jamovi Version 2.2.5.0 and verified using R.[28,29] Analysis of sex between groups was assessed using a chi-squared test of independence, analysis of age was completed using a one-way analysis of variance (ANOVA). For all statistical analyses, the non-dominant (right) hemispheres in right-handed controls were compared to the lesioned hemispheres of the PS groups. Data normality was assessed using the Shapiro-Wilk test. Between-group differences of FA and MD in the lesioned and non-lesioned hemispheres, and differences in the AIS group based on lesion location, were assessed using one-way Analysis of Covariance (ANCOVA) adjusted for age, or Kruskal-Wallis one-way ANOVA. Subsequent pairwise comparisons were assessed using either Tukey post-hoc tests, or Dwass-Steel-Critchlow-Fligner pairwise contrasts corrected for multiple comparisons (Bonferroni). Between-hemisphere differences were assessed using paired Student's t-tests (or Mann-Whitney). Along the tract differences were examined using paired and independent T-tests. In the case of normal distribution, a Student's t-test was used, and Mann-Whitney was utilized when the sample did not meet the assumption of normality. Effect sizes calculated using Cohen's d or Rank biserial correlation based on normality.

RESULTS

Seven participants were excluded from the AIS group as visual tracts could not be reconstructed in the lesioned hemisphere. All seven of these children had lesions affecting the proximal M1 artery. In total, 94 participants were included in the analysis (N=22 AIS, N=29 PVI, N=43 TDC). There were no significant sex (χ^2_1 =0.18, p = 0.67) or age (F~(2, 91)~= 2.422, p=0.09) differences between groups.

DEMOGRAPHICS

PARTICIPANT GROUP DIFFERENCES

Tractography of the visual tracts was completed successfully for 22 children with AIS, 29 children with PVI and 43 controls with exemplars illustrated in Figure 2. Compared with TDCs, children with AIS had significantly lower FA ($F_{2,91}$=30.26, p<0.001), and higher MD (χ^2_2 =35.6, p<0.001) in the lesioned hemisphere, along with lower FA ($F_{3,90}$=27.41, p<0.001) and no difference in MD ($F_{2,91}$=0.05, p=1.000) in the non-lesioned hemisphere (Figure 3). Comparing AIS to PVI, children with AIS had lower FA ($F_{2,91}$=30.26, p=0.011) and higher MD (χ^2_2 =35.6, p<0.001) in the lesioned hemisphere, with no differences in the non-lesioned hemisphere (FA = ($F_{3,90}$=27.41, p=1.000), MD = ($F_{2,91}$=0.05, p=1.000)). Comparing PVI to TDCs, FA was lower in both the lesioned ($F_{2,91}$=30.26, p<0.001) and non-lesioned ($F_{3,90}$=27.41, p<0.001) hemispheres (t_{90}=4.3, p<0.001), MD was higher in the lesioned hemisphere (χ^2_2 =35.6, p=0.007) with no difference in the non-lesioned ($F_{2,91}$=0.05, p=1.000) hemisphere.

HEMISPHERIC DIFFERENCES

The lesioned hemisphere of the AIS group showed lower FA (t_{21}=3.68, p=0.001, d=-0.817) (Figure 4) and higher MD (t_{21}=4.10, p<0.001, d=0.425) compared to non-lesioned hemisphere, whereas children with PVI showed higher MD (V_{28}=330.00, p=0.02, d=0.558) in the lesioned hemisphere compared to non-lesioned, but no between hemisphere differences in FA (t_{28}=0.22, p=0.829, d=-0.282). Interhemispheric differences for the control group were not significant for FA (t_{42}=1.97, p=0.06, d=-0.302), but did show higher MD in the non-dominant (right) hemisphere (t_{42}=4.95, p<0.001, d=-0.755).

ALONG THE TRACT GROUP DIFFERENCES

Consistent differences throughout the tracts were observed in the lesioned hemisphere (Figure 5B). FA was lower in the AIS group (p<0.001) compared to TDC along the entire tract (ROIs 2-10), whereas FA in the PVI group was lower in the anterior portion of the tract (p=0.03 to p<0.001) at ROIs 0-4 and again at ROI 7 when compared to TDC. Children with AIS had lower FA at ROIs 3 and 5-10 (p=0.008 to p<0.001) in the lesioned hemisphere and lower FA at ROIs 1, 7 and 8 (p=0.01 to p=0.03) in the non-lesioned hemisphere when compared to children with PVI. In the non-lesioned hemisphere (Figure 5C), differences in FA between stroke and TDC groups were observed at several locations. FA in both AIS and PVI was lower ($F_{2,88}$=4.19, p<0.001) compared to TDC at the optic chiasm (ROI 0). PVI showed

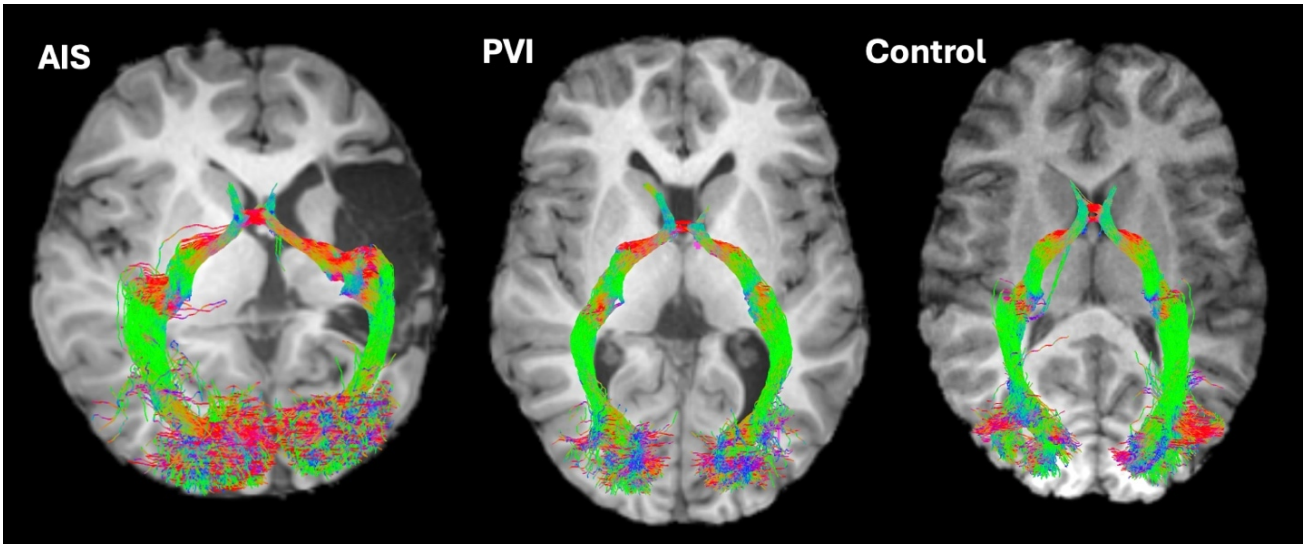

Figure 2. Visual representations of tractography in the optic tracts and optic radiations of the participant groups. These visualizations are typical examples of participants with PVI and controls and show an example of some of the asymmetry of tracts observed in AIS participants with larger lesions.

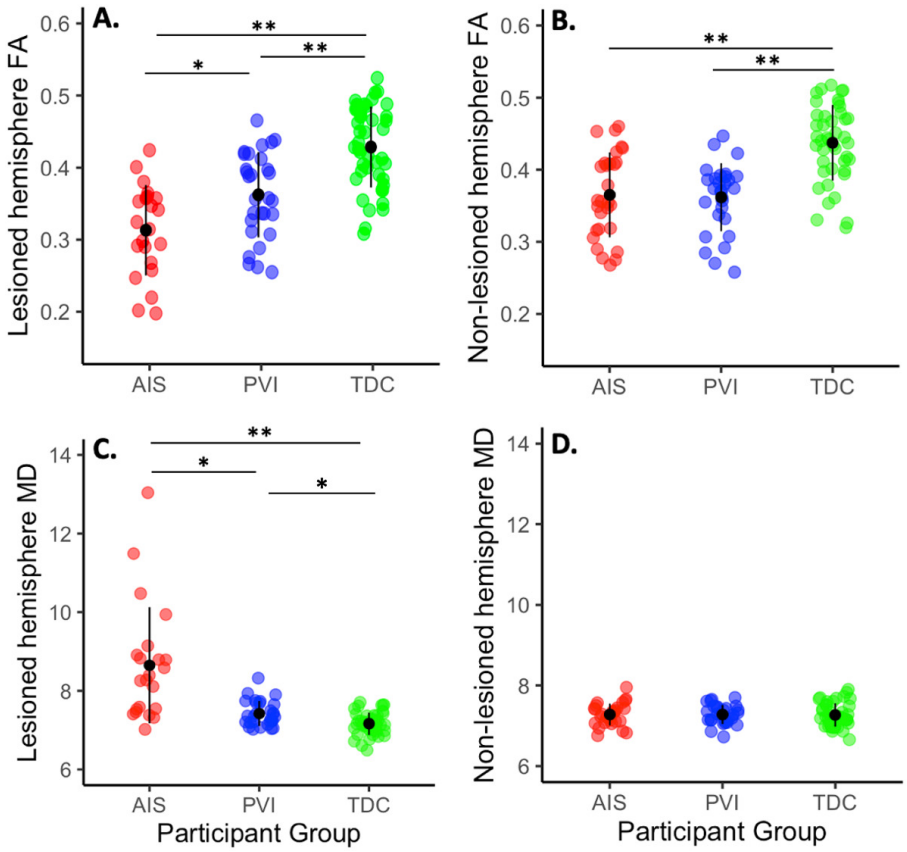

Figure 3. Vertical scatterplots illustrating group differences in microstructure between the three participant groups for each hemisphere. Fractional anisotropy in the lesioned (A) and non-lesioned (B) and hemispheres was lowest in the AIS group. Mean diffusivity in was highest in the AIS group in the lesioned hemisphere (C), with no difference between groups in the non-lesioned hemisphere (D). AIS - arterial ischemic stroke, PVI periventricular venous infarction, TDC - typically developing controls. MD values are x10^{-4}. **p<0.001, *p<0.05

lower FA compared to TDC anterior to the LGN at ROI 2 ($F_{2,88}$=5.48, p=0.004), whereas AIS showed lower FA at ROI 4 ($F_{2,88}$=0.49, p=0.03), and ROI 8 ($F_{2,88}$=1.45, p=0.005) when compared with TDCs.

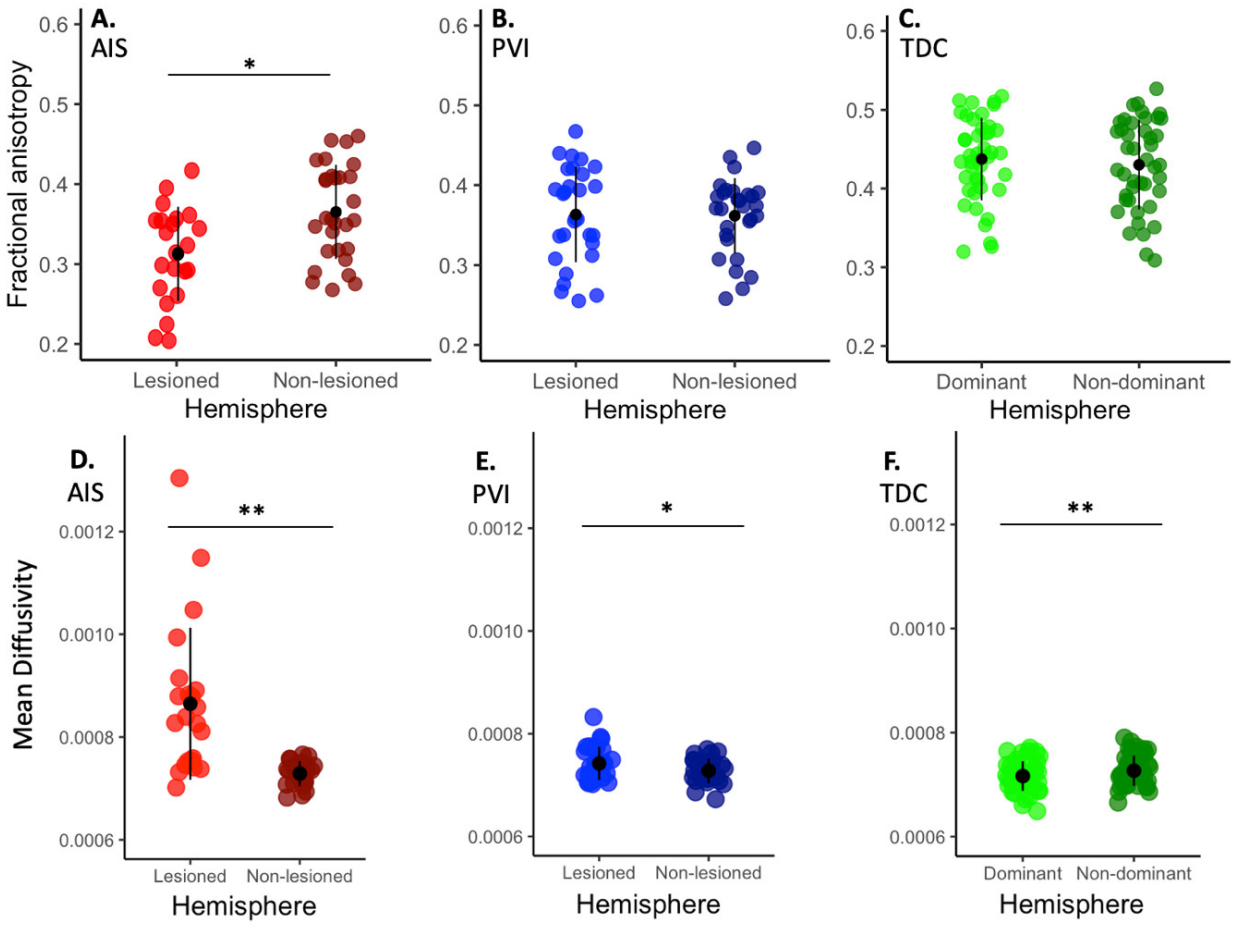

Figure 4. Vertical scatterplots illustrating hemispheric differences in fractional anisotropy (A. AIS, B. PVI, C. TDC) and mean diffusivity (D. AIS, E. PVI, F. TDC) for the three participant groups. As our TDC sample was right-handed the right hemisphere was considered non-dominant. AIS - arterial ischemic stroke, PVI periventricular venous infarction, TDC - typically developing controls. **p<0.001, *p<0.05.

Children with AIS showed higher MD throughout most of the posterior portion of the tracts at ROIs 4-10 (p=0.009 to p<0.001) in the lesioned hemisphere and the non-lesioned hemisphere (p=0.01 to p<0.001 at ROIs 1, 3 and ROIs 7-9) compared to TDCs. Children with PVI had higher MD (p=0.03 to p<0.001) at ROIs 0, 6 and 10 compared to TDCs. There were no significant differences in MD between participants with PVI and AIS in the non-lesioned hemisphere, AIS had higher MD (p=0.02 to p<0.001) than PVI at ROIs 4-10.

BETWEEN HEMISPHERE DIFFERENCES OF AIS AND PVI GROUPS ALONG THE TRACT

Participants in the AIS group had significantly lower FA and higher MD (between p<0.01 and p<0.001) in all sampled subsegments along the entirety of the tract in the lesioned hemisphere compared to the non-lesioned hemisphere. In the PVI group, between hemisphere differences of lower FA and higher MD (between p<0.02 and p<0.001) were found in the LGN and the sections just anterior and posterior to the LGN (ROIs 4 through 7), but no interhemispheric differences existed along other parts of the optic tract or optic radiations. TDCs showed higher FA (p<0.001) and lower MD (p=0.001) in the LGN of the left hemisphere (ROI 5,), and lower MD in the optic radiations of the right hemisphere (ROIs 6-9, p-values between p=0.007 and p<0.001).

BETWEEN HEMISPHERE COMPARISON WITHIN AIS GROUP

There were no differences in FA in the lesioned (t_{18}=2.00, p=0.061, d=0.892) or non-lesioned hemisphere (t_{18}=1.34, p=0.198, d=0.597), nor MD in either hemisphere (lesioned t_{18}=0.087, p=0.932, d=0.04, non-lesioned t_{18}=1.250, p=0.430, d=0.506). In both AIS and PVI groups, children with left hemisphere injuries (mean 51.2cm^3) had larger lesion volumes than right hemisphere lesions (mean 32.2cm^3).

DISCUSSION

Our results confirmed our hypothesis that the structural development of the visual white matter pathways is more likely to be altered in children with AIS, showing lower FA and higher MD, when compared to PVI and TDCs. Consis-

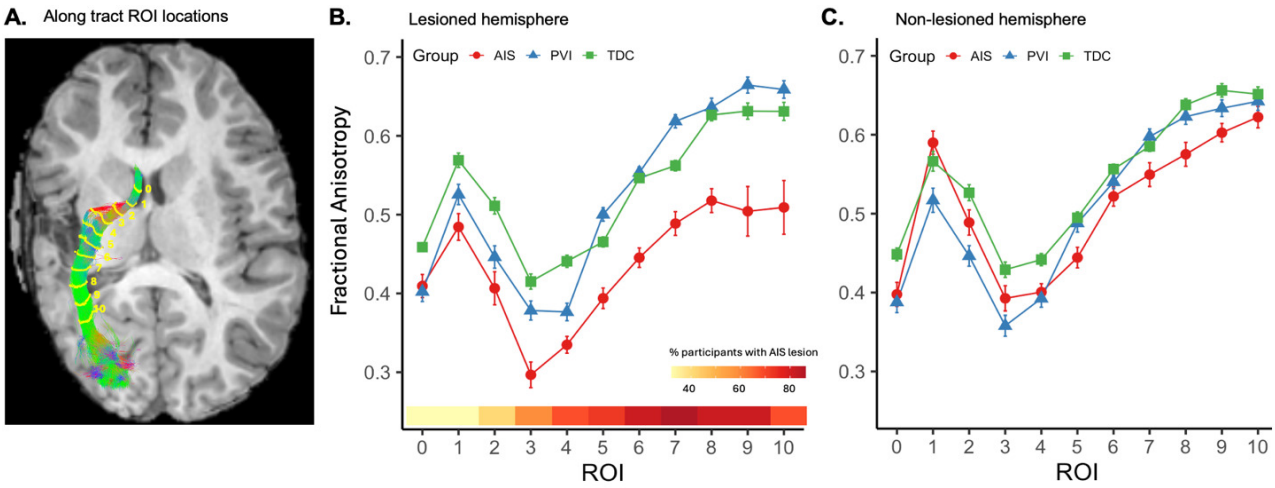

Figure 5. A) Ten sample locations along the tract starting from the optic chiasm (ROI 0), through the lateral geniculate nucleus (LGN ROI 3-4), and towards the visual cortex. Selection of underlying image was optimized to show lesion location and entirety of tract was overlaid without cropping to displayed slice. Line graphs of along the tract samples for the AIS, PVI and TDC groups in the lesioned B) and non-lesioned (C) hemispheres. Error bars denote standard error. The heat map in (B) shows more than 70% of participants with AIS had lesions located adjacent to the tracts along ROIs 5-9.

tent differences in diffusion microstructure characteristics between the AIS, PVI and TDC groups were found in both the lesioned hemisphere and the seemingly intact non-lesioned hemisphere. Along the tract analyses suggested varying microstructural alterations along the visual tracts between the AIS and PVI groups.

Perhaps the most interesting findings are the microstructural alterations that occurred in the non-lesioned hemisphere, with the most significant differences observed in the AIS population. This is consistent with previously identified alterations in the non-lesioned hemisphere of children with perinatal stroke, including differences in myelination,[10] structural changes in the thalamus,[7] diffusion properties of the corticospinal tract,[30] cerebellum,[31] basal ganglia,[32] cortex,[9] and widespread alterations in the white matter connectome.[8] These alterations have been associated with type and degree of disability, suggesting clinical relevance. While previous studies have focused on the development of the motor system and motor outcomes, our results demonstrate that perinatal stroke may also affect the development of the afferent visual pathway in non-lesioned hemisphere. This is suggestive of whole-brain plastic (re)organization that occurs following early-life injury, and that white matter structural differences are also occurring in the non-lesioned hemisphere. The addition of clinical visual outcomes such as perimetry and perceptual assessments would help determine the clinical implications of these developmental changes. Future comparisons of visual and motor pathways within subjects could also provide information on potential interactions between the two systems, and its effects on functional outcomes.

Our comparison of visual pathway white matter microstructure showed lower FA and higher MD in both PS groups compared with TDCs, with the most striking differences occurring in the AIS group. Our age-matched TDC sample is comparable with current literature of whole brain white matter development[33] and provided a template with which to compare the results of the PS groups, with injuries likely to have damaged visual pathways and/or disrupted typical development of these pathways and related broader brain networks.[4] In our study, both the AIS and PVI groups showed significant alterations in FA in both the lesioned and non-lesioned hemispheres compared to TDCs. As perinatal stroke can occur between 20 weeks gestation and 28 days of postnatal life,[3] at least some of these observed microstructural differences in the visual tracts of PS participants likely reflect subsequent developmental alterations, rather than pathway destruction that would seem more likely in the static brains of adults with stroke. Developmental alterations could include cohesiveness and compactness of fibre tracts, membrane permeability or differences in axonal packing, although we are unable to specify which underlying mechanisms are occurring in this study.[34,35] These findings add to the body of evidence that describes alterations from typical development after PS, such as white matter differences in the motor system and their association with motor disability.[10,30] Future inclusion of visual and perceptual outcomes are needed to determine the association between these white matter differences and the level of functional visual performance.

The differences between AIS and PVI groups, with the AIS population showing the most significant alterations, could also be a result of lesion timing as has been previously identified.[1] PVI is thought to typically occur mid-gestation, before myelination of the optic radiations has begun.[36] In the sensorimotor system, white matter tracts may alter "around" such lesions in children with PVI.[30,37] In contrast, AIS usually occurs near birth when damage to the visual pathways and surrounding areas may limit the ability of the brain to "re-build" or "re-route" damaged tracts.[38]

White matter development of the visual pathways typically increases sharply in infancy and slows around age 6 when it starts to resemble the adult system.[39] Injuries occurring earlier in development might allow for a longer period of post-injury white matter development to occur in the visual system. As PVI occurs during mid-gestation when the visual system is less developed, this could create an additional window for developmental reorganisation after insult that is less available to children with AIS.[40,41] Another consideration is the increasingly understood vulnerability of the white matter to "development arrest" during the window of extreme prematurity where alterations in the maturational sequence of oligodendrocytes are a primary contributor to premature white matter injury.[42] Although all our PS participants were term birth, they still show evidence of this altered white matter microstructure. An interaction amongst these or other mechanisms may explain the differences we observed between AIS and PVI populations.

Lesion location may also play a role in the differences in the visual pathways we observed between stroke groups. Damage to post-geniculate pathways often seen in AIS has been linked to structural alterations and functional differences.[6,43] Children with middle cerebral artery lesions may also see damage to subcortical structures, where afferent visual information is relayed through the optic radiations to the visual cortex. PVI injuries are typically limited to the periventricular white matter, often leaving the subcortical structures undamaged.[44] In children with AIS the lesion often affects white matter and impacts the typical pathway of the optic radiations.[3] All the AIS participants in our sample had sustained MCA strokes, resulting in lesions posterior to the LGN and often affecting the typical pathway of the optic radiations. Larger and more distal arterial occlusions were also seen to affect the optic tract between the optic chiasm and LGN. PVI lesions appeared to have less of an impact on the white matter microstructure posterior to the LGN and differences were mainly seen anterior to the LGN.

Along tract statistics were used to quantify the microstructure of these different stroke types. Specifically, for the AIS group, the entire visual tract from the optic chiasm to the primary visual cortex showed lower FA and higher MD than typically developing peers. Since AIS lesions were caused by MCA infarcts in our sample, the vascular territory of these arteries covered a wide area of brain and encompassed significant individual variability. This projection of degeneration is illustrated in Figure 5 where microstructural measurements are different and more variable for the AIS group in areas remote from the primary lesion. This damage distant to the original lesions, known as diaschisis, is present in some children and not in others. Along tract statistics also show alterations in microstructure in the optic tract between the chiasm and the LGN, which has not previously been identified in the AIS population and is suggestive of retrograde degeneration from the lesion site. Along tract statistics show additional evidence of diaschisis extending away from the primary lesion and affecting areas that are functionally and structurally connected to that lesion.

Multiple limitations of our study are considered. Head motion in children is typically higher than in adults, resulting in a greater number of artifacts and can contribute to image degradation. Head motion has also been shown to be higher in children with brain injury,[45] although there are no studies on head motion specific to the PS population. Head motion between groups was not measured in this study but participants with significant head motion were excluded from our analysis. The acquired MRI data did not include any reverse phase encoding sequences and thus a synthetic b0 was generated. Placement of ROIs was completed manually. Automation of this process may be useful in larger sample sizes, but may also be challenging due to the structural variability of PS brains based on lesion location and size. The diffusion metrics used here such as FA and MD are voxel specific and thus susceptible to the issue of crossing-fibres, particularly in areas such as the lateral geniculate nucleus, through which our tracts pass. While conventional thinking may suggest that a higher FA reflects greater white matter density, interpretation should consider that factors such as fibre diameter, density, myelination, and membrane permeability may all affect the restriction of water diffusion.[34,35,46] Although we may wish to make an inference regarding connectivity, we are only able to conclude that white matter microstructural alterations are present in children with PS compared to our control group. The addition of functional visual data would provide information about whether these microstructural differences are related to functional visual outcomes. Children with PS in our population all had motor impairment, specifically symptomatic hemiparetic CP, creating a selection bias for larger and centrally located lesions that may limit generalizability to the entire PS population.

CONCLUSION

This study contributes to existing evidence that whole brain re-organization occurs after PS, including the afferent visual pathways. Our analysis is the first to identify microstructural changes in the optic tracts and optic radiations exclusively within the PS population. Additional clinical and functional outcomes in this population is required to advance our understanding of these structural changes, and the effects of developmental plasticity on visual outcomes in children with early brain injuries. Understanding the impact of these microstructural changes on function could improve clinical practice and lead to development of novel assessment and therapeutic techniques to maximize the plasticity of the developing brain to optimize outcomes for children affected by PS.

DATA AVAILABILITY STATEMENT

Data is available upon establishment of a formal data sharing agreement, approval from the authors' local ethics committee, and approval from the requesting researcher's local ethics committee.

FUNDING SOURCES

This research was funded in part by a project grant through CHILD-BRIGHT, supported by the Canadian Institutes of Health Research. Meghan Maiani is supported through the Cumming School of Medicine "Vision and stroke recovery across the lifespan" grant.

CONFLICT OF INTEREST DISCLOSURES

The authors declare that they have no competing interests.

ACKNOWLEDGEMENTS

We thank the participants and their families for making this research possible.

Submitted: July 26, 2024 CDT, Accepted: September 12, 2024 CDT

REFERENCES

1. Dunbar M, Kirton A. Perinatal Stroke. *Seminars in Pediatric Neurology*. 2019;32:100767. doi:10.1016/j.spen.2019.08.003

2. Kirton A, deVeber G. Life After Perinatal Stroke. *Stroke*. 2013;44(11):3265-3271. doi:10.1161/STROKEAHA.113.000739

3. Dunbar M, Kirton A. Perinatal stroke: mechanisms, management, and outcomes of early cerebrovascular brain injury. *The Lancet Child & Adolescent Health*. 2018;2(9):666-676. doi:10.1016/S2352-4642(18)30173-1

4. Kirton A, Metzler MJ, Craig BT, et al. Perinatal stroke: mapping and modulating developmental plasticity. *Nat Rev Neurol*. 2021;17(7):415-432. doi:10.1038/s41582-021-00503-x

5. Koenraads Y, Porro GL, Braun KPJ, Groenendaal F, de Vries LS, van der Aa NE. Prediction of visual field defects in newborn infants with perinatal arterial ischemic stroke using early MRI and DTI-based tractography of the optic radiation. *European Journal of Paediatric Neurology*. 2016;20(2):309-318. doi:10.1016/j.ejpn.2015.11.010

6. Araneda R, Ebner-Karestinos D, Dricot L, et al. Impact of early brain lesions on the optic radiations in children with cerebral palsy. *Front Neurosci*. 2022;16:924938. doi:10.3389/fnins.2022.924938

7. Craig BT, Carlson HL, Kirton A. Thalamic diaschisis following perinatal stroke is associated with clinical disability. *Neuroimage Clin*. 2019;21:101660. doi:10.1016/j.nicl.2019.101660

8. Craig BT, Kinney-Lang E, Hilderley AJ, Carlson HL, Kirton A. Structural connectivity of the sensorimotor network within the non-lesioned hemisphere of children with perinatal stroke. *Sci Rep*. 2022;12(1):3866. doi:10.1038/s41598-022-07863-4

9. Shinde K, Craig BT, Hassett J, et al. Alterations in cortical morphometry of the contralesional hemisphere in children, adolescents, and young adults with perinatal stroke. *Sci Rep*. 2023;13(1):11391. doi:10.1038/s41598-023-38185-8

10. Yu S, Carlson HL, Mineyko A, et al. Bihemispheric alterations in myelination in children following unilateral perinatal stroke. *Neuroimage Clin*. 2018;20:7-15. doi:10.1016/j.nicl.2018.06.028

11. Ego A, Lidzba K, Brovedani P, et al. Visual-perceptual impairment in children with cerebral palsy: a systematic review. *Dev Med Child Neurol*. 2015;57:46-51. doi:10.1111/dmcn.12687

12. Belmonti V, Cioni G, Berthoz A. Anticipatory control and spatial cognition in locomotion and navigation through typical development and in cerebral palsy. *Dev Med Child Neurol*. 2016;58:22-27. doi:10.1111/dmcn.13044

13. Papadopoulos K, Metsiou K, Agaliotis I. Adaptive behavior of children and adolescents with visual impairments. *Research in Developmental Disabilities*. 2011;32(3):1086-1096. doi:10.1016/j.ridd.2011.01.021

14. Tadić V, Pring L, Dale N. Are language and social communication intact in children with congenital visual impairment at school age? *Child Psychology Psychiatry*. 2010;51(6):696-705. doi:10.1111/j.1469-7610.2009.02200.x

15. Engel-Yeger B, Hamed-Daher S. Comparing participation in out of school activities between children with visual impairments, children with hearing impairments and typical peers. *Research in Developmental Disabilities*. 2013;34(10):3124-3132. doi:10.1016/j.ridd.2013.05.049

16. Cumberland PM, Rahi JS, for the UK Biobank Eye and Vision Consortium. Visual Function, Social Position, and Health and Life Chances: The UK Biobank Study. *JAMA Ophthalmol*. Published online July 28, 2016. doi:10.1001/jamaophthalmol.2016.1778

17. Cole L, Dewey D, Letourneau N, et al. Clinical characteristics, risk factors, and outcomes associated with neonatal hemorrhagic stroke: A population-based case-control study. *JAMA Pediatr*. 2017;171(3):230-238. doi:10.1001/jamapediatrics.2016.4151

18. Friston KJ. *Statistical Parametric Mapping: The Analysis of Functional Brain Images*. Academic Press; 2011.

19. Schilling KG, Blaber J, Huo Y, et al. Synthesized b0 for diffusion distortion correction (Synb0-DisCo). *Magnetic Resonance Imaging*. 2019;64:62-70. doi:10.1016/j.mri.2019.05.008

20. Tournier JD, Smith R, Raffelt D, et al. MRtrix3: A fast, flexible and open software framework for medical image processing and visualisation. *NeuroImage*. 2019;202:116137. doi:10.1016/j.neuroimage.2019.116137

21. Dhollander T, Connelly A. *A Novel Iterative Approach to Reap the Benefits of Multi-Tissue CSD from Just Single-Shell (+b=0) Diffusion MRI Data.*; 2016.

22. Dhollander T, Emsell L, Van Hecke W, Maes F, Sunaert S, Suetens P. Track Orientation Density Imaging (TODI) and Track Orientation Distribution (TOD) based tractography. *NeuroImage*. 2014;94:312-336. doi:10.1016/j.neuroimage.2013.12.047

23. Raffelt DA, Smith RE, Ridgway GR, et al. Connectivity-based fixel enhancement: Whole-brain statistical analysis of diffusion MRI measures in the presence of crossing fibres. *NeuroImage*. 2015;117:40-55. doi:10.1016/j.neuroimage.2015.05.039

24. Tournier JD, Calamante F, Connelly A. Improved probabilistic streamlines tractography by 2nd order integration over fibre orientation distributions. *Proceedings of the International Society for Magnetic Resononance Medicine*. Published online 2010:1.

25. Oishi K, Faria AV, Van Zijl PCM, Mori S. MRI atlas of human white matter. *2011*. Published online 2011.

26. Rorden C, Brett M. Stereotaxic Display of Brain Lesions. *Behavioural Neurology*. 2000;12(4):191-200. doi:10.1155/2000/421719

27. Jenkinson M, Beckmann CF, Behrens TEJ, Woolrich MW, Smith SM. FSL. *Neuroimage*. 2012;62(2):782-790. doi:10.1016/j.neuroimage.2011.09.015

28. R Core Team. R: A language and environment for statistical computing. Published online 2021.

29. The jamovi project. Jamovi. Published online 2022.

30. Kuczynski AM, Dukelow SP, Hodge JA, et al. Corticospinal tract diffusion properties and robotic visually guided reaching in children with hemiparetic cerebral palsy. *Hum Brain Mapp*. 2018;39(3):1130-1144. doi:10.1002/hbm.23904

31. Craig BT, Olsen C, Mah S, Carlson HL, Wei XC, Kirton A. Crossed Cerebellar Atrophy in Perinatal Stroke. *Stroke*. 2019;50(1):175-177. doi:10.1161/STROKEAHA.118.022423

32. Hassett J, Carlson H, Babwani A, Kirton A. Bihemispheric developmental alterations in basal ganglia volumes following unilateral perinatal stroke. *Neuroimage Clin*. 2022;35:103143. doi:10.1016/j.nicl.2022.103143

33. Lebel C, Deoni S. The development of brain white matter microstructure. *NeuroImage*. 2018;182:207-218. doi:10.1016/j.neuroimage.2017.12.097

34. Beaulieu C. The basis of anisotropic water diffusion in the nervous system - a technical review. *NMR Biomed*. 2002;15(7-8):435-455. doi:10.1002/nbm.782

35. Jones DK, Knösche TR, Turner R. White matter integrity, fiber count, and other fallacies: the do's and don'ts of diffusion MRI. *Neuroimage*. 2013;73:239-254. doi:10.1016/j.neuroimage.2012.06.081

36. De Graaf-Peters VB, Hadders-Algra M. Ontogeny of the human central nervous system: What is happening when? *Early Human Development*. 2006;82(4):257-266. doi:10.1016/j.earlhumdev.2005.10.013

37. Staudt M. (Re-)organization of the developing human brain following periventricular white matter lesions. *Neurosci Biobehav Rev*. 2007;31(8):1150-1156.

38. Staudt M. Reorganization after pre- and perinatal brain lesions. *J Anat*. 2010;217(4):469-474. doi:10.1111/j.1469-7580.2010.01262.x

39. Lebel C, Treit S, Beaulieu C. A review of diffusion MRI of typical white matter development from early childhood to young adulthood. *NMR in Biomedicine*. 2019;32(4). doi:10.1002/nbm.3778

40. Guzzetta A, Fazzi B, Mercuri E, et al. Visual function in children with hemiplegia in the first years of life. *Dev Med Child Neurol*. 2001;43(5):321-329. doi:10.1017/s0012162201000603

41. Guzzetta A, Mercuri E, Cioni G. Visual disorders in children with brain lesions: *European Journal of Paediatric Neurology*. 2001;5(3):115-119. doi:10.1053/ejpn.2001.0481

42. Inder TE, Volpe JJ, Anderson PJ. Defining the Neurologic Consequences of Preterm Birth. *N Engl J Med*. 2023;389(5):441-453. doi:10.1056/NEJMra2303347

43. Lennartsson F, Öhnell H, Jacobson L, Nilsson M. Pre- and Postnatal Damage to the Retro-Geniculate Visual Pathways Cause Retinal Degeneration Predictive for Visual Function. *Front Hum Neurosci*. 2021;15:734193. doi:10.3389/fnhum.2021.734193

44. Kirton A, DeVeber G, Pontigon AM, Macgregor D, Shroff M. Presumed perinatal ischemic stroke: Vascular classification predicts outcomes. *Ann Neurol*. 2008;63(4):436-443. doi:10.1002/ana.21334

45. Ware AL, Shukla A, Guo S, et al. Participant factors that contribute to magnetic resonance imaging motion artifacts in children with mild traumatic brain injury or orthopedic injury. *Brain Imaging and Behavior*. 2022;16(3):991-1002. doi:10.1007/s11682-021-00582-w

46. Figley CR, Uddin MN, Wong K, Kornelsen J, Puig J, Figley TD. Potential Pitfalls of Using Fractional Anisotropy, Axial Diffusivity, and Radial Diffusivity as Biomarkers of Cerebral White Matter Microstructure. *Front Neurosci*. 2022;15:799576. doi:10.3389/fnins.2021.799576

SUPPLEMENTARY MATERIALS

Supplementary Material

Download: https://apertureneuro.org/article/123922-bilateral-differences-in-structural-connectivity-of-the-afferent-visual-pathways-of-children-with-perinatal-stroke/attachment/246930.pdf